

An $O(n)$ -Algorithm for the Higher-Order Kinematics and Inverse Dynamics of Serial Manipulators using Spatial Representation of Twists

A. Müller¹

Abstract—Optimal control in general, and flatness-based control in particular, of robotic arms necessitate to compute the first and second time derivatives of the joint torques/forces required to achieve a desired motion. In view of the required computational efficiency, recursive $O(n)$ -algorithms were proposed to this end. Aiming at compact yet efficient formulations, a Lie group formulation was recently proposed, making use of body-fixed and hybrid representation of twists and wrenches. In this paper a formulation is introduced using the spatial representation. The second-order inverse dynamics algorithm is accompanied by a fourth-order forward and inverse kinematics algorithm. An advantage of all Lie group formulations is that they can be parameterized in terms of vectorial quantities that are readily available. The method is demonstrated for the 7 DOF Franka Emika Panda robot.

Index Terms—Robotic arm, serial-elastic actuators, inverse dynamics, forward kinematics, inverse kinematics, $O(n)$ -algorithm, flatness-based control, Lie group, screws

I. INTRODUCTION

VARIOUS applications of robots need the time derivatives of the inverse dynamics solution $\mathbf{Q}(t)$ for a prescribed motion $\mathbf{q}(t)$, i.e. the time derivatives of the equations of motion (EOM) of the robotic arm

$$\mathbf{Q} = \mathbf{M}(\mathbf{q}) \ddot{\mathbf{q}} + \mathbf{C}(\dot{\mathbf{q}}, \mathbf{q}) \dot{\mathbf{q}} + \mathbf{Q}^{\text{grav}}(\mathbf{q}) + \mathbf{Q}^{\text{app}}(t) \quad (1)$$

where the vector of generalized coordinates $\mathbf{q} = (q_1, \dots, q_n)^T$ comprises the joint variables, and the vector of generalized forces $\mathbf{Q} = (Q_1, \dots, Q_n)^T$ contains the joint torques/forces. \mathbf{M} and \mathbf{C} is the generalized mass and Coriolis matrix, respectively, \mathbf{Q}_{grav} represents generalized gravity forces, and \mathbf{Q}_{app} is due to end-effector (EE) loads and general external loads.

A situation where the first and second time derivatives of (1) are needed is the flatness-based control of robots equipped with serial elastic actuators (SEA) and variable stiffness actuators (VSA) [7], [11], [24]. SEA and VSA are in particular useful for the design of exoskeletons and safe humanoid robots, and generally in context of human-robot interaction. Under the assumptions stated in [29], the dynamic

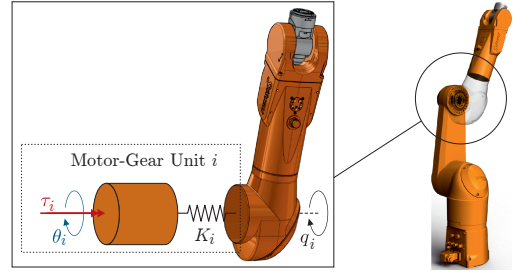


Fig. 1. Industrial robot regarded as a manipulator equipped with SEA

model of an n DOF robot actuated by SEA (Fig. 1) can be written as [7]

$$\mathbf{M}(\mathbf{q}) \ddot{\mathbf{q}} + \mathbf{C}(\dot{\mathbf{q}}, \mathbf{q}) \dot{\mathbf{q}} + \mathbf{Q}^{\text{grav}}(\mathbf{q}) + \mathbf{Q}^{\text{app}}(t) = \mathbf{K}_m(\boldsymbol{\theta} - \mathbf{q}) \quad (2)$$

$$\mathbf{M}_m(\mathbf{q}) \ddot{\boldsymbol{\theta}} + \mathbf{K}_m(\boldsymbol{\theta} - \mathbf{q}) = \boldsymbol{\tau}. \quad (3)$$

The additional second set of equations (3) governs the motor/gear dynamics, where $\boldsymbol{\theta} = (\theta_1, \dots, \theta_n)^T$ are the (rotation/translation) variables describing the motion of the motor/gear units. The mass matrix $\mathbf{M}_m = \text{diag}(M_{m,1}, \dots, M_{m,n})$ is composed of the reduced motor/gear inertias $M_{m,i}$, and $\boldsymbol{\tau}$ is the vector of motor torques/forces collocated to $\boldsymbol{\theta}$. The elastic coupling of both systems is achieved by the gear stiffness encoded in the stiffness matrix $\mathbf{K}_m = \text{diag}(K_1, \dots, K_n)$ containing the lumped stiffness parameters K_i of the motor/gear unit at joint i . The joint torques/forces acting at the robot are now determined by the elastic coupling of both systems as $\mathbf{Q} := \mathbf{K}_m(\boldsymbol{\theta} - \mathbf{q})$, and flatness-based control of robots equipped with SEA/VSA involves their first and second time derivatives.

Another application where the derivatives of the drive torques/forces are needed is the time-optimal control of standard industrial manipulators [26]. Even if the optimal control problem accounts for the limits on speed, acceleration, jerk, and drive torques/forces, the trajectories may still violate the limits on the rate of drive torques/forces, i.e. the limits on the time derivatives of the motor current set by the inverter. This requirement on the higher-order continuity of \mathbf{Q} is often overlooked, merely because time optimal motions are not yet widely applied in practice, but it is gaining importance.

Aiming at maximal computational efficiency, recursive $O(n)$ -algorithms for the evaluation of the time derivatives were reported in [2], [3], [15], [16] building upon classical Newton-Euler (NE) formulations to evaluate the EOM, where angular and translational motions are treated separately. Using

Manuscript received: August 4, 2020; Revised November 4, 2020; Accepted November 11, 2020.

This paper was recommended for publication by Editor Dezhen Song upon evaluation of the Associate Editor and Reviewers' comments. This work was supported by the LCM-K2 Center within the framework of the Austrian COMET-K2 program.

¹First Author is with Institute of Robotics, Johannes Kepler University Linz, Austria a.mueller@jku.at

Digital Object Identifier (DOI): see top of this page.

the so-called 'spatial vector' formulation, recursive algorithms were presented [8], [9], where angular and translational velocities are collectively treated as rigid body twists written as 6-vectors. Observing that twists are screws, forming the Lie algebra of the rigid body motion group $SE(3)$, these algorithms were reformulated in [25], [17]. Such Lie group algorithms are coordinate invariant, i.e. applicable regardless of the frame in which twists and wrenches are represented. It is important to remember that the 'representation' of a screw does not only regard the frame in which the vectors are resolved but also the point relative to which they are measured. From a computational point of view, the crucial point is that the number of necessary operations of the frame transformation of a screw depends on its representation. Two representations are mostly used: *body-fixed* and *spatial* representation [23], [20], [17] (Sec. II-B & Appendix B). A central feature of the Lie group (and hence of the spatial vector) formulation is the compactness of the involved expressions. A recursive algorithm for computation of the second time derivative of (1) was presented in [21] using body-fixed representations.

In the following, an $O(n)$ -algorithm for the second-order inverse dynamics is introduced, which rests on the recursive Lie group formulation of the kinematics and dynamics using the spatial representation. The algorithm comprises two recursions. Firstly, the forward kinematics run distributes the 4th-order state $(\mathbf{q}, \dot{\mathbf{q}}, \ddot{\mathbf{q}}, \ddot{\ddot{\mathbf{q}}}, \ddot{\ddot{\ddot{\mathbf{q}}}})$ among the bodies, starting from the ground. Secondly, the inverse dynamics run recursively evaluates the (spatial) momentum screws of the bodies and their time derivatives, and propagates them starting from terminal body. A salient feature of the Lie group formulation is that it admits model description in terms of readily available data without compromising computational efficiency. This paper shall complement the Lie group formulations of the recursive inverse dynamics algorithms in body-fixed and hybrid representation [21], and thus provide the starting point for research addressing the computationally most efficient as well as (regarding the parameterization and simplicity) the most user-friendly approach.

The paper is organized as follows. Sec. II recalls the Lie group modeling of robot kinematics. Sec. III presents the 4th-order forward kinematics in spatial representation of twists. The recursive 4th-order forward kinematics is combined with the inverse kinematics solution in Sec. IV. The inverse dynamics algorithm is derived in Sec. V, and its features are briefly discussed. Simulation results are presented in Sec. VI for the Franka Emika Panda robot, along with a preliminary comparison of the spatial and body-fixed algorithm. The paper closes with suggestions for future work in Sec. VII.

II. MANIPULATOR KINEMATICS

A. Manipulator configuration via the POE

A stationary robotic arm is modeled as a simple kinematic chain comprising n rigid bodies connected to the ground by n 1-DOF helical (revolute, screw, prismatic) joints. The pose of body i is represented by a homogenous transformation matrix \mathbf{C}_i in (32). More precisely, \mathbf{C}_i describes the transformation

from a body-fixed reference frame (RFR) \mathcal{F}_i , which is kinematically representing body i , to a world-fixed inertia frame (IFR).

Denote with $\mathbf{q} \in \mathbb{V}^n$ the vector of joint variables $q_i, i = 1, \dots, n$, with $\mathbb{V}^n = \mathbb{T}^{n_r} \times \mathbb{R}^{n_p}$, where n_r and n_p is the number of revolute/screw and prismatic joints, respectively. For a given vector of joint variables $\mathbf{q} \in \mathbb{V}^n$, the configuration of link i can be expressed as $\mathbf{C}_i(\mathbf{q}) = f_i(\mathbf{q}) \mathbf{A}_i$ using the product of exponentials (POE) in the form [20], [22]

$$f_i(\mathbf{q}) = \exp(\mathbf{Y}_1 q_1) \exp(\mathbf{Y}_2 q_2) \dots \exp(\mathbf{Y}_i q_i), \quad (4)$$

which was introduced in [1] and is now a central element in modern robotics [17], [23]. The POE (4) describes the relative configuration of the RFR \mathcal{F}_i at body i relative to its location at $\mathbf{q} = \mathbf{0}$, while $\mathbf{A}_i := \mathbf{C}_i(\mathbf{0}) \in SE(3)$ is the absolute reference configuration of the body-fixed frame w.r.t. to the IFR in this zero-reference configuration. In the above POE, the joint kinematics is encoded in the screw coordinate vectors $\mathbf{Y}_j \in \mathbb{R}^6$ represented in the IFR. The screw coordinates for a revolute joint j are $\mathbf{Y}_j = (\mathbf{e}_j, \mathbf{y}_j \times \mathbf{e}_j)^T$, where \mathbf{e}_j is a unit vector along the screw axis, and \mathbf{y}_j is the position vector to a point on the revolute joint axis measured and resolved in the IFR. The screw coordinate vector for a prismatic joint is $\mathbf{Y}_j = (\mathbf{e}_j, \mathbf{0})^T$, while for a screw joint with pitch h_j , this is $\mathbf{Y}_j = (\mathbf{e}_j, \mathbf{y}_j \times \mathbf{e}_j + h_j \mathbf{e}_j)^T$. These screw coordinates allow using geometric information and vectorial quantities, deduced from an arbitrary IFR.

Remark 1: The Denavit-Hartenberg (DH) convention is frequently used to describe the manipulator geometry. The DH-parameters for joint j are denoted with $\alpha_j, a_j, d_j, \vartheta_j$ [30]. With the DH-convention, the absolute reference configuration is determined as

$$\mathbf{A}_i = \mathbf{A}_{i-1} \text{Rot}(\vartheta_i) \text{Trans}(d_i) \text{Trans}(a_i) \text{Rot}(\alpha_i) \quad (5)$$

with $\mathbf{A}_0 = \mathbf{I}$, and with DH parameter values according to the reference configuration. The homogenous transformation matrices $\text{Rot}(\varphi)$ and $\text{Trans}(x)$ describe a pure rotation and translation, respectively, about/along the joint axis according to the DH-convention [17].

B. Manipulator velocities and Jacobian in spatial representation

The twist $\mathbf{V}_i^s = (\boldsymbol{\omega}_i^s, \mathbf{v}_i^s)^T$ of link i in spatial representation comprises the angular velocity $\boldsymbol{\omega}_i^s$ of \mathcal{F}_i relative to \mathcal{F}_0 , and the translational velocity \mathbf{v}_i^s of the body-fixed point momentarily coinciding with the origin of \mathcal{F}_0 , where both vectors are resolved in \mathcal{F}_0 . It is determined recursively by [17], [19]

$$\mathbf{V}_i^s = \mathbf{V}_{i-1}^s + \mathbf{S}_i \dot{q}_i, \quad i = 1, \dots, n \quad (6)$$

with $\mathbf{V}_0^s = \mathbf{0}$, where $\mathbf{S}_i \in \mathbb{R}^6$ is the instantaneous joint screw coordinate vector of joint i . The latter is determined from the joint screw coordinates \mathbf{Y}_j in the reference configuration by the frame transformation according to the motion of body j , according to (4), as

$$\mathbf{S}_j(\mathbf{q}) = \mathbf{A} \mathbf{d}_{f_j(\mathbf{q})} \mathbf{Y}_j, \quad j \leq i \quad (7)$$

where the adjoint operator \mathbf{Ad}_C in (33) describes the transformation of screw coordinates according to the frame transform $C \in SE(3)$ [23], [27]. The EE is attached to the terminal body n , and w.l.o.g. the twist of the terminal body is identified with the EE-twist, $\mathbf{V}_E^s := \mathbf{V}_n^s$. For the EE/terminal body n , the recursive summation (6) can be summarized as

$$\mathbf{V}_E^s = \mathbf{J}\dot{\mathbf{q}} \quad \text{with} \quad \mathbf{J}(\mathbf{q}) := \left(\mathbf{S}_1(\mathbf{q}) \mid \cdots \mid \mathbf{S}_n(\mathbf{q}) \right) \quad (8)$$

where \mathbf{J} is the *spatial Jacobian* of the robotic arm. This is the geometric Jacobian [28] of the robotic arm that determines the EE-twist in spatial representation (with the joint screws \mathbf{S}_j in spatial representation). The geometric Jacobian that determines the EE-twist in body-fixed representation is called the *body-fixed Jacobian* [20].

In contrast to the recursive relation in terms of body-fixed twists (see (40) in Appendix B), the relation (6) does not involve frame transformations of twists. However, the screw coordinates \mathbf{S}_j are not constant and must be computed with (7), so that both formulations involve a similar number of operations.

III. FOURTH-ORDER FORWARD KINEMATICS

The recursion (6) solves the first-order forward kinematics problem of the *robot mechanism*, which consists in determining the state of all bodies of the robot mechanism for given state $(\mathbf{q}, \dot{\mathbf{q}})$, whereas (8) solves the forward kinematics problem of the *robot manipulator*. Now, the second-order derivatives of the EOM (1) involve the 4th-order time derivatives of $\mathbf{q}(t)$, and a recursive evaluation requires solution of the 4th-order forward kinematics problem, which is to determine the velocity, acceleration, jerk, and jounce of all bodies for given $\mathbf{q}, \dot{\mathbf{q}}, \ddot{\mathbf{q}}, \overset{\cdot\cdot}{\mathbf{q}}$. This needs time derivatives of \mathbf{S}_i . The latter is given as $\dot{\mathbf{S}}_i = \mathbf{ad}_{\mathbf{V}_i^s} \mathbf{S}_i$, where \mathbf{ad} is the 'screw product' matrix in (37). Repeated application of this, along with (6), and using the \mathbf{ad} matrix in (37), yields [22]

$$\begin{aligned} \dot{\mathbf{S}}_i &= \mathbf{ad}_{\mathbf{V}_i^s} \mathbf{S}_i, \quad \ddot{\mathbf{S}}_i = (\mathbf{ad}_{\dot{\mathbf{V}}_i^s} + \mathbf{ad}_{\mathbf{V}_i^s}^2) \mathbf{S}_i \\ \overset{\cdot\cdot}{\mathbf{S}}_i &= (\mathbf{ad}_{\ddot{\mathbf{V}}_i^s} + 2\mathbf{ad}_{\dot{\mathbf{V}}_i^s} \mathbf{ad}_{\mathbf{V}_i^s} + \mathbf{ad}_{\mathbf{V}_i^s} \mathbf{ad}_{\dot{\mathbf{V}}_i^s} + \mathbf{ad}_{\mathbf{V}_i^s}^3) \mathbf{S}_i. \end{aligned} \quad (9)$$

This gives rise to the recursive $O(n)$ -algorithm 1 for the 4th-order forward kinematics for the robot mechanism where for the ground body ($i = 0$) $\mathbf{V}_0^s = \dot{\mathbf{V}}_0^s = \ddot{\mathbf{V}}_0^s = \mathbf{0}$, and $f_0 = \mathbf{I}$. In order to account for gravity, the ground acceleration is set to $\dot{\mathbf{V}}_0^s = \mathbf{G}_0^s = (\mathbf{0}, -\mathbf{g})^T$ with the gravitational acceleration vector $\mathbf{g} \in \mathbb{R}^3$ represented in the IFR. The instantaneous screw coordinates \mathbf{S}_i and their time derivatives will be reused in the inverse dynamics recursion.

IV. COMBINED FOURTH-ORDER INVERSE AND FORWARD KINEMATICS RECURSION

The above forward kinematics run assumes that the trajectory $\mathbf{q}(t)$ and its derivatives are known. If the motion is not determined up-front in terms of joint variables (e.g. as a result of optimal motion planning in joint space), it will have to be determined from a prescribed EE-motion, which necessitates solving the *inverse kinematics problem of the manipulator*. The higher-order inverse kinematics is addressed in the following

Algorithm 1: 4th-Order Forward Kinematics Recursion

Input: $\mathbf{q}, \dot{\mathbf{q}}, \ddot{\mathbf{q}}, \overset{\cdot\cdot}{\mathbf{q}}, \overset{\cdot\cdot\cdot}{\mathbf{q}}$, and $\mathbf{Y}_i, i = 1, \dots, n$

For $i = 1, \dots, n$ do

$$f_i = f_{i-1} \exp(\mathbf{Y}_i \mathbf{q}_i) \quad \text{Position kinematics}$$

$$\mathbf{C}_i = f_i \mathbf{A}_i$$

$$\mathbf{S}_i = \mathbf{Ad}_{f_i(\mathbf{q})} \mathbf{Y}_i \quad \text{Higher-order kinematics}$$

$$\mathbf{V}_i^s = \mathbf{V}_{i-1}^s + \mathbf{S}_i \dot{\mathbf{q}}_i$$

$$\dot{\mathbf{S}}_i = \mathbf{ad}_{\mathbf{V}_i^s} \mathbf{S}_i$$

$$\dot{\mathbf{V}}_i^s = \dot{\mathbf{V}}_{i-1}^s + \mathbf{S}_i \ddot{\mathbf{q}}_i + \dot{\mathbf{S}}_i \dot{\mathbf{q}}_i$$

$$\ddot{\mathbf{S}}_i = (\mathbf{ad}_{\dot{\mathbf{V}}_i^s} + \mathbf{ad}_{\mathbf{V}_i^s}^2) \mathbf{S}_i$$

$$\ddot{\mathbf{V}}_i^s = \ddot{\mathbf{V}}_{i-1}^s + \mathbf{S}_i \overset{\cdot\cdot}{\mathbf{q}}_i + 2\dot{\mathbf{S}}_i \dot{\mathbf{q}}_i + \ddot{\mathbf{S}}_i \dot{\mathbf{q}}_i$$

$$\overset{\cdot\cdot}{\mathbf{S}}_i = (\mathbf{ad}_{\ddot{\mathbf{V}}_i^s} + 2\mathbf{ad}_{\dot{\mathbf{V}}_i^s} \mathbf{ad}_{\mathbf{V}_i^s} + \mathbf{ad}_{\mathbf{V}_i^s} \mathbf{ad}_{\dot{\mathbf{V}}_i^s} + \mathbf{ad}_{\mathbf{V}_i^s}^3) \mathbf{S}_i$$

$$\overset{\cdot\cdot\cdot}{\mathbf{V}}_i^s = \overset{\cdot\cdot\cdot}{\mathbf{V}}_{i-1}^s + \mathbf{S}_i \overset{\cdot\cdot\cdot}{\mathbf{q}}_i + 3\dot{\mathbf{S}}_i \overset{\cdot\cdot}{\mathbf{q}}_i + 3\ddot{\mathbf{S}}_i \dot{\mathbf{q}}_i + \overset{\cdot\cdot\cdot}{\mathbf{S}}_i \dot{\mathbf{q}}_i$$

End

Output: $\mathbf{V}_i^s, \dot{\mathbf{V}}_i^s, \ddot{\mathbf{V}}_i^s, \overset{\cdot\cdot}{\mathbf{V}}_i^s$ and $\mathbf{S}_i, \dot{\mathbf{S}}_i, \ddot{\mathbf{S}}_i, \overset{\cdot\cdot}{\mathbf{S}}_i$

for kinematically non-redundant manipulators, where \mathbf{J} is a $n \times n$ matrix. The geometric inverse kinematics problem can be solved numerically using closed-loop inverse kinematics (CLIK) algorithms [6] or with a Newton iteration scheme using the inverse of \mathbf{J} .

Remark 2: The inverse kinematics solution can also be used for kinematically redundant robots when the joint space decomposition is used, which was proposed in [31], and used for trajectory planning in [10], [18]. Details of the higher-order inverse kinematics in closed form can be found in [26].

The solution to the 1st-order (velocity) inverse kinematics problem of a non-redundant robot follows from (8) as $\dot{\mathbf{q}} = \mathbf{J}_E^{-1} \mathbf{V}_E^s$, presumed that it is not in a forward kinematic singularity. The EE-acceleration can be expressed as $\dot{\mathbf{V}}_E^s = \mathbf{J}\ddot{\mathbf{q}} + \sum_{i \leq n} \dot{\mathbf{S}}_i \dot{\mathbf{q}}_i$, and the solution for the 2nd-order (acceleration) inverse kinematics problem is $\ddot{\mathbf{q}} = \mathbf{J}^{-1} (\dot{\mathbf{V}}_E^s - \sum_{i \leq n} \dot{\mathbf{S}}_i \dot{\mathbf{q}}_i)$. The expressions for the jerk and jounce are similar. The above expressions (9) for the derivatives of \mathbf{S}_i could be inserted to yield closed form solutions [22], but it is computationally more efficient to compute and reuse them.

The relation for $\mathbf{q}^{(k)}$ involves the first $k-1$ time derivative of the EE-twist \mathbf{V}_E^s and, via (9), the derivatives of the twists \mathbf{V}_i^s of up to order $k-2$ of all bodies. Thus, solving the manipulator inverse kinematics of order k presupposes the solution of the forward kinematics of the mechanism up to order $k-1$. These steps are summarized in Algorithm 2. The Jacobian inverse $\mathbf{J}^{-1}(\mathbf{q})$ is only computed once in step 2.a). The terms $\dot{\mathbf{S}}_i \dot{\mathbf{q}}_i$ from 3a) can be reused in 3b), $\ddot{\mathbf{S}}_i \dot{\mathbf{q}}_i, \dot{\mathbf{S}}_i \ddot{\mathbf{q}}_i$ from 4a) in 4b), and $\overset{\cdot\cdot}{\mathbf{S}}_i \overset{\cdot\cdot}{\mathbf{q}}_i, \overset{\cdot\cdot\cdot}{\mathbf{S}}_i \overset{\cdot\cdot}{\mathbf{q}}_i, \overset{\cdot\cdot\cdot}{\mathbf{S}}_i \dot{\mathbf{q}}_i$ from 5.a) in 5.b).

V. HIGHER-ORDER INVERSE DYNAMICS

A. Spatial NE-equations and their time derivatives

Consider a free-floating rigid body whose pose relative to the IFR is described by $C \in SE(3)$. Its spatial momentum co-screw

$$\mathbf{\Pi}^s = \mathbf{M}^s \mathbf{V}^s \in se^* \quad (3) \quad (10)$$

is determined by the *spatial mass matrix*

$$\mathbf{M}^s = \begin{pmatrix} \Theta^s & m(\tilde{\mathbf{d}} + \tilde{\mathbf{r}}) \\ -m(\tilde{\mathbf{d}} + \tilde{\mathbf{r}}) & m\mathbf{I} \end{pmatrix}. \quad (11)$$

Algorithm 2:
Combined inverse and forward kinematics recursion

Input: \mathbf{q} , \mathbf{V}_E^s , $\dot{\mathbf{V}}_E^s$, $\ddot{\mathbf{V}}_E^s$, and $\mathbf{Y}_i, i = 1, \dots, n$

1) Configurations, joint screws (EE-Jacobian):

For $i = 1, \dots, n$ do
 $f_i = f_{i-1} \exp(\mathbf{Y}_i q_i)$
 $\mathbf{C}_i = f_i \mathbf{A}_i$
 $\mathbf{S}_i = \mathbf{A} \mathbf{d}_{f_i(\mathbf{q})} \mathbf{Y}_i$
End

2.a) 1st-order inverse kinematics of manipulator:

$$\dot{\mathbf{q}} = \mathbf{J}^{-1} \mathbf{V}_E^s$$

2.b) 1st-order forward kinematics of robot mechanism:

For $i = 1, \dots, n-1$ do
 $\mathbf{V}_i^s = \mathbf{V}_{i-1}^s + \mathbf{S}_i \dot{q}_i$
 $\dot{\mathbf{S}}_i = \mathbf{ad}_{\mathbf{V}_i^s} \mathbf{S}_i$
End

3.a) 2nd-order inverse kinematics of manipulator:

$$\ddot{\mathbf{q}} = \mathbf{J}^{-1} \left(\dot{\mathbf{V}}_E^s - \sum_{i \leq n} \dot{\mathbf{S}}_i \dot{q}_i \right)$$

3.b) 2nd-order forward kinematics of robot mechanism:

For $i = 1, \dots, n-1$ do
 $\dot{\mathbf{V}}_i^s = \mathbf{V}_{i-1}^s + \mathbf{S}_i \ddot{q}_i + \dot{\mathbf{S}}_i \dot{q}_i$
 $\ddot{\mathbf{S}}_i = (\mathbf{ad}_{\dot{\mathbf{V}}_i^s} + \mathbf{ad}_{\mathbf{V}_i^s}^2) \mathbf{S}_i$
End

4.a) 3rd-order inverse kinematics of manipulator:

$$\ddot{\mathbf{q}} = \mathbf{J}^{-1} \left(\ddot{\mathbf{V}}_E^s - \sum_{i \leq n} (2\dot{\mathbf{S}}_i \ddot{q}_i + \ddot{\mathbf{S}}_i \dot{q}_i) \right)$$

4.b) 3rd-order forward kinematics of robot mechanism:

For $i = 1, \dots, n-1$ do
 $\ddot{\mathbf{V}}_i^s = \ddot{\mathbf{V}}_{i-1}^s + \mathbf{S}_i \ddot{\ddot{q}}_i + 2\dot{\mathbf{S}}_i \ddot{q}_i + \ddot{\mathbf{S}}_i \dot{q}_i$
 $\ddot{\mathbf{S}}_i = (\mathbf{ad}_{\dot{\mathbf{V}}_i^s} + 2\mathbf{ad}_{\mathbf{V}_i^s} \mathbf{ad}_{\dot{\mathbf{V}}_i^s} + \mathbf{ad}_{\mathbf{V}_i^s} \mathbf{ad}_{\mathbf{V}_i^s} + \mathbf{ad}_{\mathbf{V}_i^s}^3) \mathbf{S}_i$
End

5.a) 4th-order inverse kinematics of manipulator:

$$\ddot{\mathbf{q}} = \mathbf{J}^{-1} \left(\ddot{\mathbf{V}}_E^s - \sum_{i \leq n} (\ddot{\mathbf{S}}_i \ddot{\ddot{q}}_i + 3\dot{\mathbf{S}}_i \ddot{\ddot{q}}_i + \ddot{\mathbf{S}}_i \dot{\ddot{q}}_i) \right)$$

5.b) 4th-order forward kinematics of robot mechanism:

For $i = 1, \dots, n-1$ do
 $\ddot{\mathbf{V}}_i^s = \ddot{\mathbf{V}}_{i-1}^s + \mathbf{S}_i \ddot{\ddot{\ddot{q}}}_i + 3\dot{\mathbf{S}}_i \ddot{\ddot{\ddot{q}}}_i + 3\ddot{\mathbf{S}}_i \dot{\ddot{\ddot{q}}}_i + \ddot{\mathbf{S}}_i \ddot{\ddot{\ddot{q}}}_i$
End

Output: $\dot{\mathbf{q}}, \ddot{\mathbf{q}}, \ddot{\mathbf{q}}, \ddot{\mathbf{q}}, \dot{\mathbf{S}}_i, \ddot{\mathbf{S}}_i, \ddot{\mathbf{S}}_i, \mathbf{V}_i^s, \dot{\mathbf{V}}_i^s, \ddot{\mathbf{V}}_i^s, \mathbf{J}(\mathbf{q})$

Therein, $\mathbf{r} \in \mathbb{R}^3$ is the position vector of the body-fixed frame, and $\mathbf{d} \in \mathbb{R}^3$ is the vector from the body-fixed frame to the COM, both resolved in IFR, and Θ^s is the inertia tensor, resolved in IFR, w.r.t. the body-fixed point which instantaneously coincides with the IFR origin. The spatial mass matrix is configuration dependent. The mass matrix is constant if it is represented in the body-fixed frame \mathcal{F}_b . This *body-fixed mass matrix* has the form

$$\mathbf{M}^b = \begin{pmatrix} \Theta^b & {}^b \mathbf{d} m \\ -{}^b \tilde{\mathbf{d}} m & \mathbf{I} m \end{pmatrix}. \quad (12)$$

where ${}^b \mathbf{d}$ is the vector from the origin of the body-fixed frame to the COM resolved in body-fixed frame, and Θ^b is the constant inertia tensor w.r.t. the body-fixed frame. The two representations are related via [20]

$$\mathbf{M}^s = \mathbf{A} \mathbf{d}_C^{-T} \mathbf{M}^b \mathbf{A} \mathbf{d}_C^{-1}. \quad (13)$$

Along with relation (39), this yields the time derivative

$$\dot{\mathbf{M}}^s = -\mathbf{M}^s \mathbf{ad}_{\mathbf{V}^s} - \mathbf{ad}_{\dot{\mathbf{V}}^s}^T \mathbf{M}^s. \quad (14)$$

The momentum balance yields the spatial representation of the Newton-Euler (NE) equations

$$\dot{\mathbf{\Pi}}^s + \mathbf{W}^{s,app} + \mathbf{W}^{s,grav} = \mathbf{0} \quad (15)$$

where $\mathbf{W}^{s,grav}$ is the wrench due to gravity and $\mathbf{W}^{s,app}$ the wrench due to general external loads applied to the body. Inserting (10), and using (14), yields the NE-equations in terms of the spatial twist and acceleration

$$\mathbf{M}^s \dot{\mathbf{V}}^s - \mathbf{ad}_{\dot{\mathbf{V}}^s}^T \mathbf{M}^s \mathbf{V}^s + \mathbf{W}^{s,app} + \mathbf{W}^{s,grav} = \mathbf{0}. \quad (16)$$

The time derivative of the NE-equations (16) yields the rate of the spatial wrench in the dynamic equilibrium (15)

$$\ddot{\mathbf{\Pi}}^s + \dot{\mathbf{W}}^{s,app} + \dot{\mathbf{W}}^{s,grav} = \mathbf{0}. \quad (17)$$

Evaluation of (17) necessitates the second time derivative of the spatial momentum screw. This derivative is obtained, with the explicit relation (14) for the time derivative of the spatial mass matrix, as

$$\begin{aligned} \ddot{\mathbf{\Pi}}^s &= \mathbf{M}^s \ddot{\mathbf{V}}^s + \dot{\mathbf{M}}^s \dot{\mathbf{V}}^s - \mathbf{ad}_{\dot{\mathbf{V}}^s}^T \dot{\mathbf{\Pi}}^s - \mathbf{ad}_{\mathbf{V}^s}^T \ddot{\mathbf{\Pi}}^s \\ &= \mathbf{M}^s (\ddot{\mathbf{V}}^s - \mathbf{ad}_{\dot{\mathbf{V}}^s} \dot{\mathbf{V}}^s) - \mathbf{ad}_{\dot{\mathbf{V}}^s}^T \dot{\mathbf{\Pi}}^s - \mathbf{ad}_{\mathbf{V}^s}^T (\dot{\mathbf{\Pi}}^s + \mathbf{M}^s \dot{\mathbf{V}}^s). \end{aligned} \quad (18)$$

Inserting $\mathbf{M}^s \dot{\mathbf{V}}^s = \dot{\mathbf{\Pi}}^s + \mathbf{ad}_{\mathbf{V}^s}^T \dot{\mathbf{\Pi}}^s$ and rearranging terms yields

$$\ddot{\mathbf{\Pi}}^s = \mathbf{M}^s (\ddot{\mathbf{V}}^s - \mathbf{ad}_{\dot{\mathbf{V}}^s} \dot{\mathbf{V}}^s) - 2\mathbf{ad}_{\dot{\mathbf{V}}^s}^T \dot{\mathbf{\Pi}}^s - (\mathbf{ad}_{\mathbf{V}^s} + \mathbf{ad}_{\dot{\mathbf{V}}^s}^2)^T \dot{\mathbf{\Pi}}^s. \quad (19)$$

The expression (19) allows calculating the second time derivative of the spatial momentum screw from the momentum and its first derivative.

A further time derivative of the NE-equations (15) determines the second derivative of the spatial wrench

$$\ddot{\mathbf{\Pi}}^s + \ddot{\mathbf{W}}^{s,app} + \ddot{\mathbf{W}}^{s,grav} = \mathbf{0}. \quad (20)$$

Starting from (19) the third derivative of $\mathbf{\Pi}^s$ is

$$\begin{aligned} \ddot{\mathbf{\Pi}}^s &= \mathbf{M}^s (\ddot{\mathbf{V}}^s - 2\mathbf{ad}_{\dot{\mathbf{V}}^s} \dot{\mathbf{V}}^s + \mathbf{ad}_{\dot{\mathbf{V}}^s}^2 \dot{\mathbf{V}}^s) - 2\mathbf{ad}_{\dot{\mathbf{V}}^s}^T \ddot{\mathbf{\Pi}}^s \\ &\quad - \mathbf{ad}_{\mathbf{V}^s}^T \dot{\mathbf{M}}^s (\dot{\mathbf{V}}^s - \mathbf{ad}_{\mathbf{V}^s} \dot{\mathbf{V}}^s) - (3\mathbf{ad}_{\dot{\mathbf{V}}^s} + \mathbf{ad}_{\mathbf{V}^s}^2)^T \dot{\mathbf{\Pi}}^s \\ &\quad - (\mathbf{ad}_{\dot{\mathbf{V}}^s} + \mathbf{ad}_{\mathbf{V}^s} \mathbf{ad}_{\dot{\mathbf{V}}^s} + \mathbf{ad}_{\mathbf{V}^s} \mathbf{ad}_{\mathbf{V}^s})^T \dot{\mathbf{\Pi}}^s. \end{aligned} \quad (21)$$

Solving (19) for $\mathbf{M}^s (\ddot{\mathbf{V}}^s - \mathbf{ad}_{\dot{\mathbf{V}}^s} \dot{\mathbf{V}}^s)$ and replacing this in (21) leads to the final form of the third time derivative

$$\begin{aligned} \ddot{\mathbf{\Pi}}^s &= \mathbf{M}^s (\ddot{\mathbf{V}}^s - 2\mathbf{ad}_{\dot{\mathbf{V}}^s} \dot{\mathbf{V}}^s + \mathbf{ad}_{\dot{\mathbf{V}}^s}^2 \dot{\mathbf{V}}^s) \\ &\quad - 3\mathbf{ad}_{\dot{\mathbf{V}}^s}^T \ddot{\mathbf{\Pi}}^s - 3(\mathbf{ad}_{\mathbf{V}^s} + \mathbf{ad}_{\dot{\mathbf{V}}^s}^2)^T \dot{\mathbf{\Pi}}^s \\ &\quad - (\mathbf{ad}_{\dot{\mathbf{V}}^s} + 2\mathbf{ad}_{\mathbf{V}^s} \mathbf{ad}_{\dot{\mathbf{V}}^s} + \mathbf{ad}_{\mathbf{V}^s} \mathbf{ad}_{\mathbf{V}^s} + \mathbf{ad}_{\mathbf{V}^s}^3)^T \dot{\mathbf{\Pi}}^s. \end{aligned} \quad (22)$$

In the expressions (15), (19), (22), the derivatives of $\mathbf{\Pi}^s$ could be expressed in terms of \mathbf{V}^s and its time derivatives. This is not shown since it is computationally more efficient to reuse the derivatives of $\mathbf{\Pi}^s$.

B. End-effector loads and applied wrenches

The manipulator is subjected to external loads, and in particular interacts with the environment via the EE. The corresponding EE-wrenches are due to the (possibly time-varying) inertia of the object being manipulated or due to contact, for instance. With the assumption that the reference frame \mathcal{F}_n of the terminal link is located at the EE, the EE-load contributes an applied wrench $\mathbf{W}_n^{\text{s,app}}(t)$ at the terminal link. Further general loads acting on the remaining bodies are included in the model by $\mathbf{W}_i^{\text{s,app}}(t)$, $i = 1, \dots, n-1$ if they are known.

EE-loads are not included in the recursive higher-order inverse dynamics algorithms reported in the literature. This is motivated by the fact that measuring them directly requires force/torque sensors collocated at the EE, but moreover estimating their time derivatives is difficult [14]. Nevertheless, for control purposes it is important to include EE-loads, and their time derivatives whenever possible.

C. Gravity loads

If the effect of gravity is of interest (e.g. for design purpose), the gravity wrench and its time derivatives can be determined separately. The wrench at body i due to gravity in spatial representation is

$$\mathbf{W}_i^{\text{s,grav}} = \mathbf{Ad}_{\mathbf{C}_i}^{-T} \mathbf{M}_i^{\text{b}} \mathbf{Ad}_{\mathbf{C}_i}^{-1} \mathbf{G}_i^{\text{s}} = \mathbf{M}_i^{\text{s}} \mathbf{G}_i^{\text{s}}. \quad (23)$$

Time derivatives of this gravity wrench follow immediately with repeated application of (14) as

$$\dot{\mathbf{W}}_i^{\text{s,grav}} = -(\mathbf{M}_i^{\text{s}} \mathbf{ad}_{\mathbf{v}_i^{\text{s}}} + \mathbf{ad}_{\mathbf{v}_i^{\text{s}}}^T \mathbf{M}_i^{\text{s}}) \mathbf{G}_i^{\text{s}} \quad (24)$$

$$\begin{aligned} \ddot{\mathbf{W}}_i^{\text{s,grav}} = & \left((\mathbf{M}_i^{\text{s}} \mathbf{ad}_{\mathbf{v}_i^{\text{s}}}^2 + \mathbf{ad}_{\mathbf{v}_i^{\text{s}}}^T \mathbf{M}_i^{\text{s}} \mathbf{ad}_{\mathbf{v}_i^{\text{s}}} + \mathbf{M}_i^{\text{s}} \mathbf{ad}_{\mathbf{v}_i^{\text{s}}}) \right. \\ & \left. + (\mathbf{M}_i^{\text{s}} \mathbf{ad}_{\mathbf{v}_i^{\text{s}}}^2 + \mathbf{ad}_{\mathbf{v}_i^{\text{s}}}^T \mathbf{M}_i^{\text{s}} \mathbf{ad}_{\mathbf{v}_i^{\text{s}}} + \mathbf{M}_i^{\text{s}} \mathbf{ad}_{\mathbf{v}_i^{\text{s}}})^T \right) \mathbf{G}_i^{\text{s}}. \end{aligned} \quad (25)$$

The relations (23)-(25) can be evaluated within the forward kinematics recursion (Algorithm 1).

D. Generalized forces and their derivatives

The NE-equations (15) govern the dynamics of the individual unconstrained bodies. When bodies are regarded as part of the manipulator, the NE-equations are

$$\dot{\mathbf{\Pi}}_i^{\text{s}} + \mathbf{W}_i^{\text{s,app}} + \mathbf{W}_i^{\text{s,grav}} = \mathbf{W}_i^{\text{s}} \quad (26)$$

where \mathbf{W}_i^{s} accounts for constraint reactions as well as joint forces/torques in the 'free directions'. Applying Jourdain's principle of virtual power, along with the kinematic relation (6), yields

$$\begin{aligned} \delta \mathbf{v}_i^{\text{s}T} \mathbf{W}_i^{\text{s}} &= \delta \mathbf{v}_i^{\text{s}T} (\dot{\mathbf{\Pi}}_i^{\text{s}} + \mathbf{W}_i^{\text{s,app}} + \mathbf{W}_i^{\text{s,grav}}) \quad (27) \\ \sum_{j=1}^i \delta q_j \mathbf{S}_j^T \mathbf{W}_i^{\text{s}} &= \sum_{j=1}^i \delta q_j \mathbf{S}_j^T (\dot{\mathbf{\Pi}}_i^{\text{s}} + \mathbf{W}_i^{\text{s,app}} + \mathbf{W}_i^{\text{s,grav}}). \end{aligned}$$

Rearranging relation (27) according to q_i yields

$$\delta q_i \mathbf{S}_i^T \sum_{j=i}^n \mathbf{W}_j^{\text{s}} = \delta q_i \mathbf{S}_i^T \sum_{j=i}^n (\dot{\mathbf{\Pi}}_j^{\text{s}} + \mathbf{W}_j^{\text{s,app}} + \mathbf{W}_j^{\text{s,grav}}). \quad (28)$$

The generalized forces $Q_i := \mathbf{S}_i^T (\mathbf{W}_i^{\text{s}} + \dots + \mathbf{W}_n^{\text{s}})$ are thus determined by

$$Q_i = \mathbf{S}_i^T (\dot{\mathbf{\Pi}}_i^{\text{s}} + \mathbf{W}_i^{\text{s,app}} + \mathbf{W}_i^{\text{s,grav}} + \bar{\mathbf{W}}_{i+1}^{\text{s}}) \quad (29)$$

where

$$\bar{\mathbf{W}}_i^{\text{s}} := \bar{\mathbf{W}}_{i+1}^{\text{s}} + \dot{\mathbf{\Pi}}_i^{\text{s}} + \mathbf{W}_i^{\text{s,app}} + \mathbf{W}_i^{\text{s,grav}} \quad (30)$$

are the interbody-wrenches due to the (actuated) motion of the kinematic chain from body i to the terminal body n , with $\bar{\mathbf{W}}_{n+1}^{\text{s}} = \mathbf{0}$. The term $\mathbf{S}_i^T \bar{\mathbf{W}}_i^{\text{s}}$ should be interpreted as reciprocal product of twist (in ray coordinates) and wrench (in axis coordinates). The time derivatives of the generalized forces are thus

$$\begin{aligned} \dot{Q}_i &= \mathbf{S}_i^T \dot{\bar{\mathbf{W}}}_i^{\text{s}} + \dot{\mathbf{S}}_i^T \bar{\mathbf{W}}_i^{\text{s}} \quad (31) \\ \ddot{Q}_i &= \mathbf{S}_i^T \ddot{\bar{\mathbf{W}}}_i^{\text{s}} + \ddot{\mathbf{S}}_i^T \bar{\mathbf{W}}_i^{\text{s}} + 2\dot{\mathbf{S}}_i^T \dot{\bar{\mathbf{W}}}_i^{\text{s}} \end{aligned}$$

E. Inverse dynamics algorithm

After execution of the recursive forward kinematics Algorithm 1 (or Algorithm 2 if the inverse kinematics is not already solved) the configuration, spatial twist, acceleration, jerk, and jounce of each individual body are computed. Additionally, the instantaneous joint screws \mathbf{S}_i and their time derivatives are available. This data provides the input for the inverse dynamics run. The second-order inverse dynamics computes the generalized forces \mathbf{Q} , i.e. joint forces/torques, and their first and second time derivatives needed to perform a desired motion $\mathbf{q}(t)$. The relations (31) and (30) together with (15), (19), (22) and (23), (24), (25) give rise to the backward recursion listed as Algorithm 3 solving the inverse dynamics problem. The spatial momentum and its time derivatives are used as intermediate variables. If available, in addition to the data computed by the forward kinematics recursion, the applied wrenches, and in particular the wrench due to EE-loads, is supplied to Algorithm 3. While the momenta $\mathbf{\Pi}_i^{\text{s}}$ and inter-body wrenches $\bar{\mathbf{W}}_i^{\text{s}}$, and their time derivatives, are basically algorithmic variables they can be used to monitor the manipulator.

F. Features of the algorithm

The basic difference of the spatial formulation, in contrast to the body-fixed formulation (see Appendix B), is that the recursions (6) and (30) do not involve frame transformations of twists or wrenches. This is obvious comparing (6) with (40), and (30) with (41). However, in the spatial formulation (6), the instantaneous joint screw coordinates \mathbf{S}_i must be computed by a frame transformation of \mathbf{Y}_i , while the ${}^i\mathbf{X}_i$ in (40) are constant. Further, in (16) the mass matrix is not constant and must be computed according to (13). Therefore the spatial and body-fixed versions are computationally equivalent. A detailed analysis can be found in [9] where it is shown that the body-fixed formulation requires slightly less numerical operations. This argument does not carry over to the higher-order algorithms, however, since the joint screws \mathbf{S}_i and the mass matrices \mathbf{M}_i^{s} are reused in the higher-order relations of Algorithm 1 and 2, and no frame transformations of the

Algorithm 3: 2nd-Order Inverse Dynamics Recursion

Input: $C_i, V_i^s, \dot{V}_i^s, \ddot{V}_i^s, \bar{V}_i^s, S_i, \dot{S}_i, \ddot{S}_i, \bar{S}_i, i = 1, \dots, n$
 $\bar{W}_i^{s,app}, \dot{\bar{W}}_i^{s,app}, \ddot{\bar{W}}_i^{s,app}, i = 1, \dots, n; \bar{V}_0^s$

For $i = n, \dots, 1$ do

$$\begin{aligned} M_i^s &= \text{Ad}_{C_i}^{-T} M_i^b \text{Ad}_{C_i} \\ \Pi_i^s &= M_i^s V_i^s \\ \dot{\Pi}_i^s &= M_i^s \dot{V}_i^s - \text{ad}_{V_i^s}^T \Pi_i^s \\ \ddot{\Pi}_i^s &= M_i^s (\ddot{V}_i^s - \text{ad}_{V_i^s} \dot{V}_i^s) \\ &\quad - 2\text{ad}_{V_i^s}^T \dot{\Pi}_i^s - (\text{ad}_{V_i^s} + \text{ad}_{V_i^s}^2)^T \Pi_i^s \\ \ddot{\Pi}_i^s &= M_i^s (\ddot{V}_i^s - 2\text{ad}_{V_i^s} \dot{V}_i^s + \text{ad}_{V_i^s}^2 V_i^s) \\ &\quad - 3\text{ad}_{V_i^s}^T \dot{\Pi}_i^s - 3(\text{ad}_{V_i^s} + \text{ad}_{V_i^s}^2)^T \dot{\Pi}_i^s \\ &\quad - (\text{ad}_{V_i^s} + 2\text{ad}_{V_i^s} \text{ad}_{V_i^s} + \text{ad}_{V_i^s}^3)^T \Pi_i^s \\ \bar{W}_i^s &= \bar{W}_{i+1}^s + \dot{\Pi}_i^s + \bar{W}_i^{s,app} \\ \dot{\bar{W}}_i^s &= \dot{\bar{W}}_{i+1}^s + \ddot{\Pi}_i^s + \dot{\bar{W}}_i^{s,app} \\ \ddot{\bar{W}}_i^s &= \ddot{\bar{W}}_{i+1}^s + \ddot{\Pi}_i^s + \ddot{\bar{W}}_i^{s,app} \\ Q_i &= S_i^T \bar{W}_i^s \\ \dot{Q}_i &= \dot{S}_i^T \bar{W}_i^s + \ddot{S}_i^T \bar{W}_i^s \\ \ddot{Q}_i &= \ddot{S}_i^T \bar{W}_i^s + \dot{S}_i^T \dot{\bar{W}}_i^s + 2\dot{S}_i^T \dot{\bar{W}}_i^s \end{aligned}$$

End

Output: $Q_i, \dot{Q}_i, \ddot{Q}_i$ and inter-body wrenches $\bar{W}_i^s, \dot{\bar{W}}_i^s, \ddot{\bar{W}}_i^s$

time derivatives of V_i^s and \bar{W}_i^s are necessary. Compared with the algorithm in body-fixed representation (Appendix B), computing the time derivatives \dot{Q}_i, \ddot{Q}_i is slightly more expensive as it involves two, respectively three scalar products. Also the time derivatives of the NE-equations involve an additional term.

The higher-order algorithm inherits the basic features of the Lie group formulations for robot kinematics and dynamics [17], [19], [20]. The most advantageous feature of this geometric formulation is the frame-invariant parameterization in terms of vectorial quantities. This allows, for instance, processing data in universal robotic description format (URDF), which describe joint and link kinematics in terms of position vectors and rotation matrices [32], [17].

VI. EXAMPLE: FRANKA EMIKA PANDA

The Franka Emika Panda is a redundant 7 DOF robotic arm. Its dynamic parameters were reported in [12]. In the zero reference configuration, shown in Fig. 1 of [12], the unit vectors along the joint axes, resolved in the IFR \mathcal{F}_0 , are

$$\begin{aligned} \mathbf{e}_1 = \mathbf{e}_3 = \mathbf{e}_5 &= (0, 0, 1)^T, \mathbf{e}_2 = (0, 1, 0)^T \\ \mathbf{e}_4 = \mathbf{e}_6 &= (0, -1, 0)^T, \mathbf{e}_7 = (0, 0, -1)^T \end{aligned}$$

and the position vectors to the joint axes are

$$\begin{aligned} \mathbf{y}_1 &= (0, 0, d_1)^T, \mathbf{y}_3 = (0, 0, d_1 + d_3)^T, \mathbf{y}_4 = (a_4, 0, d_1 + d_3)^T \\ \mathbf{y}_5 &= (0, 0, d_1 + d_3 + d_5)^T, \mathbf{y}_7 = (a_7, 0, d_1 + d_3 + d_5)^T, \end{aligned}$$

and $\mathbf{y}_2 = \mathbf{y}_1, \mathbf{y}_6 = \mathbf{y}_5$. The geometric parameters given in the data sheet are $d_1 = 0.333\text{m}, d_3 = 0.316\text{m}, d_5 = 0.384\text{m},$

$a_4 = 0.0825\text{m}, a_7 = 0.088\text{m}$. The spatial screw coordinates according to $\mathbf{Y}_j = (\mathbf{e}_j, \mathbf{y}_j)^T$ are thus

$$\begin{aligned} \mathbf{Y}_1 &= \mathbf{Y}_3 = \mathbf{Y}_5 = (0, 0, 1, 0, 0, 0)^T \\ \mathbf{Y}_2 &= (0, 1, 0, -d_1, 0, 0)^T, \mathbf{Y}_4 = (0, -1, 0, d_1 + d_3, 0, -a_4)^T \\ \mathbf{Y}_6 &= (0, -1, 0, d_1 + d_3 + d_5, 0, 0)^T, \mathbf{Y}_7 = (0, 0, -1, 0, a_7, 0)^T. \end{aligned}$$

Body-fixed reference frames are defined as indicated in Fig. 1 of [12]. They are located at the joints so that the \mathbf{y}_i are also position vectors to the reference frames. The reference configuration of the bodies are

$$\begin{aligned} \mathbf{A}_1 &= \begin{pmatrix} 1 & 0 & 0 & 0 \\ 0 & 1 & 0 & 0 \\ 0 & 0 & 1 & 0.333 \\ 0 & 0 & 0 & 1 \end{pmatrix}, \mathbf{A}_2 = \begin{pmatrix} 1 & 0 & 0 & 0 \\ 0 & 0 & 1 & 0 \\ 0 & -1 & 0 & 0.333 \\ 0 & 0 & 0 & 1 \end{pmatrix} \\ \mathbf{A}_3 &= \begin{pmatrix} 1 & 0 & 0 & 0 \\ 0 & 1 & 0 & 0 \\ 0 & 0 & 1 & 0.649 \\ 0 & 0 & 0 & 1 \end{pmatrix}, \mathbf{A}_4 = \begin{pmatrix} 1 & 0 & 0 & 0.0825 \\ 0 & 0 & -1 & 0 \\ 0 & 1 & 0 & 0.649 \\ 0 & 0 & 0 & 1 \end{pmatrix} \\ \mathbf{A}_5 &= \begin{pmatrix} 1 & 0 & 0 & 0 \\ 0 & 1 & 0 & 0 \\ 0 & 0 & 1 & 1.033 \\ 0 & 0 & 0 & 1 \end{pmatrix}, \mathbf{A}_6 = \begin{pmatrix} 1 & 0 & 0 & 0 \\ 0 & 0 & -1 & 0 \\ 0 & 1 & 0 & 1.033 \\ 0 & 0 & 0 & 1 \end{pmatrix} \\ \mathbf{A}_7 &= \begin{pmatrix} 1 & 0 & 0 & 0.088 \\ 0 & -1 & 0 & 0 \\ 0 & 0 & -1 & 1.033 \\ 0 & 0 & 0 & 1 \end{pmatrix} \end{aligned}$$

The dynamic parameters (mass, COM, inertia) w.r.t. to the body-fixed frames are taken from Tables VIII and IX of the supplementary document to [12].

The spatial forward kinematics algorithm 1 and the inverse dynamics algorithm 3 have been implemented in Matlab. Also implemented was the body-fixed version of the recursive algorithm from [21]. The code and example scripts are available as supplementary Multimedia Material. The second-order inverse dynamics was solved for the validation trajectory $\mathbf{q}(t)$ defined by (31) in [12]. This allows direct comparison with results reported in [12], which can be reproduced using the toolbox referred to in [12]. The inverse kinematics algorithm 2 could be used if the EE motion is given, rather than the joint trajectory. To this end, one could resort to the joint space decomposition since the Panda robot is kinematically redundant. Note that friction was not included for all computations. Figure 2 shows the joint torques Q_i and their derivatives \dot{Q}_i, \ddot{Q}_i . The results were validated against the solution computed from the closed form analytic expressions of the EOM and their analytic derivatives.

As a preliminary comparison of the computational performance, the execution times for 40000 evaluation calls of the Matlab code for the presented spatial formulation and for the body-fixed algorithm [21] were determined. On a PC (i5-9500, 3GHz) running MS-Windows, the spatial algorithm needed 7.15 s and the body-fixed 8.36 s, i.e. the spatial is 15% faster. These preliminary results are not representative, however, since the timing includes computational overhead and also Matlab's run time optimization. A reliable comparison would necessitate a dedicated stand-alone implementation, preferably on a real-time system.

VII. CONCLUSION AND SUGGESTED FUTURE RESEARCH

The proposed recursive formulation for the second-order inverse dynamics and the fourth-order forward kinematics

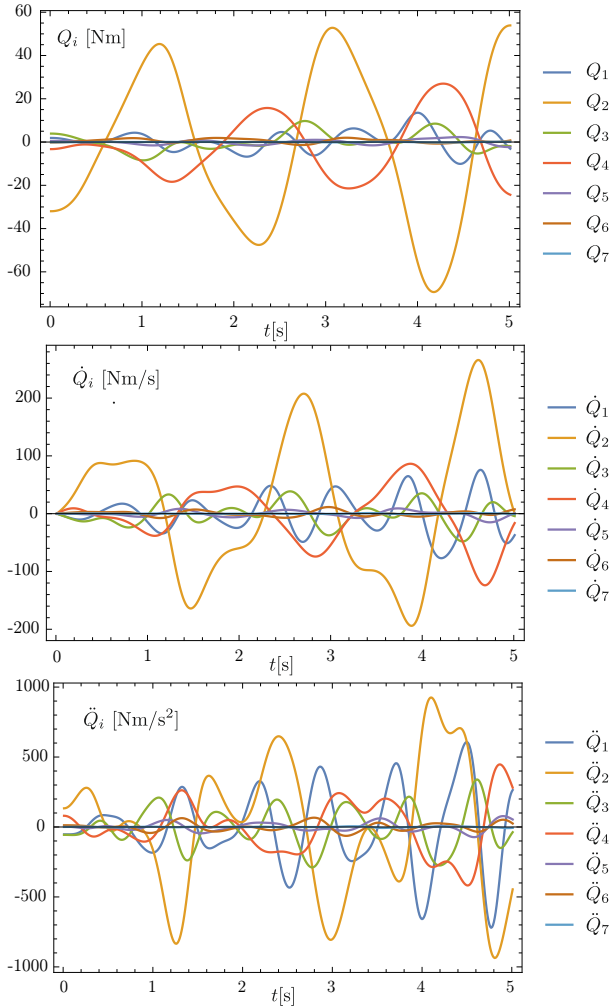


Fig. 2. Joint torques Q_i and their first and second derivatives, \dot{Q}_i and \ddot{Q}_i , for the validation trajectory according to equation (31) in [12].

allow for implementation of computationally efficient $O(n)$ algorithms. The presented algorithm in spatial representation complements the Lie group formulation in body-fixed and hybrid representation reported in [21]. Therewith, second order inverse-dynamics $O(n)$ algorithms are now available for the three relevant representations of spatial objects. This provides the basis for an exhaustive comparison and investigation into their computational efficiency *and* their user-friendliness. Moreover, in contrast to the formulations using classical vector algebra, the Lie group formulation provides an alternative that is compact, and easy to maintain and implement, which parallels the EOM Lie group formulations [17], [20]. When rolled out and written in terms of the 3-vector notation, the body-fixed formulation [21] gives exactly the relations presented in [2], [3], [15], [16]. It should also be remarked that the actual representation (spatial, body-fixed, hybrid) of spatial objects (twists, wrenches, inertias) is rather an algorithmic feature but is not apparent to the user. The results for Q_i and their derivatives are indeed independent from the representation.

Future work will be focused on detailed analysis and comparison of the complexity of the respective formulation.

Special emphasis will be given on computationally efficient implementations making repeated use of terms as well as minimizing matrix-vector operations. Only then a final conclusion as to which representation leads to the most efficient algorithm can be drawn. An important aspect of the implementation will be to reduce accumulation of errors due to the computation with finite precision. The latter could be an issue in particular for the higher-order inverse dynamics since the numerical values of Q_i , \dot{Q}_i , and \ddot{Q}_i have a different order of magnitude. Another topic will be the higher-order partial derivatives of the EOM w.r.t. generalized coordinates q_i . Such first-order derivatives (using body-fixed representation) were presented in [4], [5]. All formulations should be compared with automatic differentiation methods [13].

APPENDIX A SCREWS AND RIGID BODY MOTIONS

In the following, basic concepts are recalled as far as necessary for the paper. Details can be found in [17], [23], [27].

Rigid body configurations are represented by homogenous transformation matrices that form the Lie group $SE(3)$. The configuration of body i , i.e. the configuration of its body-fixed frame \mathcal{F}_i w.r.t., the IFR, is then denoted by the matrix

$$\mathbf{C}_i = \begin{pmatrix} \mathbf{R}_i & \mathbf{r}_i \\ \mathbf{0} & 1 \end{pmatrix} \in SE(3) \quad (32)$$

with rotation matrix $\mathbf{R}_i \in SO(3)$ and position vector $\mathbf{r}_i \in \mathbb{R}^3$. The time evolution of $\mathbf{C}_i(t)$ describes the spatial motion.

Rigid body twists and wrenches are coordinate invariant objects. Twists are screws that form the Lie algebra $se(3)$ and wrenches are co-screws forming the dual $se^*(3)$. In a chosen reference frame, both are represented as 6-vectors. Twists $\mathbf{V} = (\boldsymbol{\omega}, \mathbf{v})^T$ are represented in ray coordinates, and wrenches $\mathbf{W} = (\mathbf{m}, \mathbf{f})^T$ in axis coordinates. Denote with ${}^i\mathbf{X} \in \mathbb{R}^6$ the screw coordinate vector represented in body-fixed frame \mathcal{F}_i and with $\mathbf{X} \in \mathbb{R}^6$ its representation in the spatial IFR. Screw coordinate vectors transform from body-fixed to spatial representation according to $\mathbf{X} = \text{Ad}_{\mathbf{C}_i} {}^i\mathbf{X}$, with

$$\text{Ad}_{\mathbf{C}_i} = \begin{pmatrix} \mathbf{R}_i & \mathbf{0} \\ \tilde{\mathbf{r}}_i \mathbf{R}_i & \mathbf{R}_i \end{pmatrix}. \quad (33)$$

The corresponding transformation of co-screws (wrenches) is ${}^i\mathbf{W} = \text{Ad}_{\mathbf{C}_i}^T \mathbf{W}$, where ${}^i\mathbf{W}, \mathbf{W} \in se^*(3)$ is the co-screw coordinate vector in body-fixed and spatial representation, respectively. The time derivative of screw and co-screw coordinates represented in moving frame \mathcal{F}_i is, respectively,

$$\text{Ad}_{\mathbf{C}_i}^{-1} \dot{\mathbf{X}} = {}^i\dot{\mathbf{X}} + \text{ad}_{\mathbf{v}_i} {}^i\mathbf{X}, \quad \text{for } \mathbf{X} \in se(3) \quad (34)$$

$$\text{Ad}_{\mathbf{C}_i}^T \dot{\mathbf{W}} = {}^i\dot{\mathbf{W}} - \text{ad}_{\tilde{\mathbf{v}}_i}^T {}^i\mathbf{W}, \quad \text{for } \mathbf{W} \in se^*(3) \quad (35)$$

Denote with $\mathbf{X} = (\boldsymbol{\xi}, \boldsymbol{\eta})^T$ a general screw coordinate vector. The Lie bracket (screw product) is given as

$$[\mathbf{X}_1, \mathbf{X}_2] = (\boldsymbol{\xi}_1 \times \boldsymbol{\xi}_2, \boldsymbol{\eta}_1 \times \boldsymbol{\xi}_2 + \boldsymbol{\xi}_1 \times \boldsymbol{\eta}_2)^T = \text{ad}_{\mathbf{X}_1} \mathbf{X}_2 \quad (36)$$

with the matrix

$$\text{ad}_{\mathbf{x}} = \begin{pmatrix} \tilde{\boldsymbol{\xi}} & \mathbf{0} \\ \tilde{\boldsymbol{\eta}} & \tilde{\boldsymbol{\xi}} \end{pmatrix}. \quad (37)$$

This operation is occasionally called the 'generalized cross product' [9]. The time derivative of the adjoint transformation matrix and its inverse is

$$\dot{\text{Ad}}_{\mathbf{C}} = \text{ad}_{\mathbf{v}_s} \text{Ad}_{\mathbf{C}} \quad (38)$$

$$\text{Ad}_{\mathbf{C}}^{-1} = -\text{Ad}_{\mathbf{C}}^{-1} \text{ad}_{\mathbf{v}_s} \quad (39)$$

APPENDIX B

MAIN STEPS OF THE BODY-FIXED $O(n)$ ALGORITHM

Here some basic recursive relations of the body-fixed algorithm reported in [21] are shown for comparison. The twist of body i in body-fixed representation is the aggregate $\mathbf{V}_i^b = (\boldsymbol{\omega}_i^b, \mathbf{v}_i^b)^T$ of the angular velocity $\boldsymbol{\omega}_i^b$ of a body-fixed frame \mathcal{F}_i relative to a world frame \mathcal{F}_0 , and the translational velocity \mathbf{v}_i^b of the origin of \mathcal{F}_i relative to \mathcal{F}_0 , where both vectors are resolved in \mathcal{F}_i . It is related to the spatial representation by $\mathbf{V}_i^s = \text{Ad}_{\mathbf{C}_i} \mathbf{V}_i^b$. The velocities and accelerations are determined in the forward kinematics run as (${}^i\mathbf{X}_i$ are constant screw coordinates of joint i represented in the body-fixed frame)

$$\mathbf{V}_i^b = \text{Ad}_{\mathbf{C}_{i,i-1}} \mathbf{V}_{i-1}^b + {}^i\mathbf{X}_i \dot{q}_i \quad (40)$$

$$\dot{\mathbf{V}}_i^b = \text{Ad}_{\mathbf{C}_{i,i-1}} \dot{\mathbf{V}}_{i-1}^b + \dot{q}_i \text{ad}_{\mathbf{V}_i^b} {}^i\mathbf{X}_i + {}^i\mathbf{X}_i \ddot{q}_i.$$

The jerk and jounce recursions are omitted. The inter-body wrenches and their first time derivatives are calculated with

$$\bar{\mathbf{W}}_i^b = \text{Ad}_{\mathbf{C}_{i+1,i}}^T \bar{\mathbf{W}}_{i+1}^b + \mathbf{M}_i^b \dot{\mathbf{V}}_i^b - \text{ad}_{\mathbf{V}_i^b}^T \mathbf{M}_i^b \mathbf{V}_i^b + \mathbf{W}_i^{\text{b,app}}$$

$$\begin{aligned} \dot{\bar{\mathbf{W}}}_i^b &= \text{Ad}_{\mathbf{C}_{i+1,i}}^T (\dot{\bar{\mathbf{W}}}_{i+1}^b - \dot{q}_{i+1} \text{ad}_{\mathbf{x}_{i+1}}^T \bar{\mathbf{W}}_{i+1}^b) \\ &\quad + \mathbf{M}_i^b \dot{\dot{\mathbf{V}}}_i^b - \text{ad}_{\dot{\mathbf{V}}_i^b}^T \mathbf{M}_i^b \dot{\mathbf{V}}_i^b - \text{ad}_{\mathbf{V}_i^b}^T \mathbf{M}_i^b \mathbf{V}_i^b + \dot{\mathbf{W}}_i^{\text{b,app}} \end{aligned} \quad (41)$$

$$Q_i = {}^i\mathbf{X}_i^T \bar{\mathbf{W}}_i^b, \quad \dot{Q}_i = {}^i\mathbf{X}_i^T \dot{\bar{\mathbf{W}}}_i^b. \quad (42)$$

REFERENCES

- [1] R. W. Brockett: Robotic manipulators and the product of exponentials formula, *Mathematical Theory of Networks and Systems*, Lecture Notes in Control and Information Sciences, 58, 1984, pp. 120-129a
- [2] G. Buondonno, A. De Luca: A recursive Newton-Euler algorithm for robots with elastic joints and its application to control, 2015 IEEE/RSJ IROS, 5526-5532
- [3] G. Buondonno, A. De Luca: Efficient Computation of Inverse Dynamics and Feedback Linearization for VSA-Based Robots, *IEEE Rob. Aut. Letters*, 1(2), 2016, 908-915
- [4] J. Carpentier, N. Mansard: Analytical Derivatives of Rigid Body Dynamics Algorithms, in: *Robotics: Science and Systems (RSS 2018)*, Jun 2018, Pittsburgh, US
- [5] J. Carpentier et al.: The Pinocchio C++ library : A fast and flexible implementation of rigid body dynamics algorithms and their analytical derivatives, *IEEE/SICE International Symposium on System Integration (SII)*, Paris, France, 2019, pp. 614-619
- [6] A. Colomé and C. Torras: Closed-Loop Inverse Kinematics for Redundant Robots: Comparative Assessment and Two Enhancements, *IEEE/ASME Transactions on Mechatronics*, Vol. 20, No. 2, pp. 944-955, 2015
- [7] A. De Luca: Decoupling and feedback linearization of robots with mixed rigid/elastic joints, *Int. J. Rob. Nonlin. Cont.*, 8, 1998, 965-977 flexible joint manipulators, *Multibody Syst Dyn.* 32, 2014, 117-131
- [8] R. Featherstone: The Calculation of Robot Dynamics using Articulated-Body Inertias, *Int. J. Robotics Research*, Vol. 2, No. 1, 1983, pp. 13-30
- [9] R. Featherstone: *Rigid Body Dynamics Algorithms*, Springer, 2008

- [10] M. Galicki: Time-optimal controls of kinematically redundant manipulators with geometric constraints, *IEEE Trans. Robot. Autom.*, Vol. 16, no. 1, 2000, pp. 89-93
- [11] H. Gattringer, et al.: Recursive methods in control of flexible joint manipulators, *Multibody Syst Dyn.* 32, 2014, 117-131
- [12] C. Gaz, M. Cognetti, A. Oliva, P. Robuffo Giordano and A. De Luca, Dynamic Identification of the Franka Emika Panda Robot With Retrieval of Feasible Parameters Using Penalty-Based Optimization, *IEEE Rob. Aut. Letters*, Vol. 4, No. 4, pp. 4147-4154, 2019
- [13] M. Gifthalder et al.: Automatic Differentiation of Rigid Body Dynamics for Optimal Control and Estimation, *Advanced Robotics*, Vol. 31, No. 22, 2017, pp. 1225-1237
- [14] A. Giusti, J. Malzahn, N. G. Tsagarakis, M. Althoff: On the Combined Inverse-Dynamics/Passivity-Based Control of Elastic-Joint Robots, *IEEE Tran. Robotics*, vol. 34, no. 6, 2018, pp. 1461-1471
- [15] C. Guarino Lo Bianco, E. Fantini: A recursive Newton-Euler approach for the evaluation of generalized forces derivatives, 12th IEEE Int. Conf. Methods Models Autom. Robot., 2006, 739-744
- [16] C. Guarino Lo Bianco: Evaluation of Generalized Force Derivatives by Means of a Recursive Newton-Euler Approach, *IEEE Trans. Rob.*, 25(4), 2009, 954-959
- [17] K.M. Lynch, F.C. Park: *Modern Robotics*, Cambridge, 2017
- [18] S. Ma, M. Watanabe: Time optimal path-tracking control of kinematically redundant manipulators, *JSME Int. Journal*, Vol. 47, No. 2, 2004, pp. 582-590
- [19] A. Müller: Screw and Lie group theory in multibody dynamics – Motion representation and recursive kinematics of tree-topology systems, *Multibody Syst Dyn.*, Vol. 43, No. 1, pp. 1-34
- [20] A. Müller: Screw and Lie group theory in multibody dynamics – Recursive algorithms and equations of motion of tree-topology systems, *Multibody Syst Dyn.*, Vol. 42, No. 2, 2018, pp. 219-248
- [21] A. Müller: Recursive Second-Order Inverse Dynamics for Serial Manipulators, *IEEE Int. Conf. Robotics Automations (ICRA)*, May 29-June 3, 2017, Singapore
- [22] A. Müller: An overview of formulae for the higher-order kinematics of lower-pair chains with applications in robotics and mechanism theory, *Mech. Mach. Theory*, Vol. 142, 2019
- [23] R.M. Murray, Z. Li, and S.S. Sastry, *A Mathematical Introduction to Robotic Manipulation*, CRC Press BocaRaton, 1994
- [24] G. Palli, C. Melchiorri, A. De Luca: On the Feedback Linearization of Robots with Variable Joint Stiffness, *IEEE Int. Conf. Rob. Aut. (IROS)*, Pasadena, CA, USA, May 19-23, 2008
- [25] F. C. Park, J. E. Bobrow, S. R. Ploen: A Lie group formulation of robot dynamics, *Int. J. Rob. Research*, Vol. 14, No. 6, 1995, pp. 609-618
- [26] A. Reiter, A. Müller, H. Gattringer: On Higher-Order Inverse Kinematics Methods in Time-Optimal Trajectory Planning for Kinematically Redundant Manipulators, *IEEE Trans. Industrial Informatics*, Vol. 14, No. 4, 2018, pp. 1681 - 1690
- [27] J. Selig: *Geometric Fundamentals of Robotics (Monographs in Computer Science Series)*, Springer-Verlag New York, 2005
- [28] Siciliano, B., Sciavicco, L., Villani, L., Oriolo, G.: *Robotics*, Springer, London, 2009
- [29] M.W. Spong: Modeling and Control of Elastic Joint Robots, *ASME J. Dyn. Sys., Meas., Control*, Vol. 109, No. 4, 1987, pp. 310-318
- [30] J. J. Uicker, B. Ravani, P. N. Sheth: *Matrix Methods in the Design Analysis of Mechanisms and Multibody Systems*, Cambridge University Press, 2013.
- [31] C. Wampler: Inverse kinematic functions for redundant manipulators, *IEEE Int. Conf. Robot. Autom.*, 1987, pp. 610-617
- [32] Robot Operating System (ROS), Open Source Robotics Foundation, accessed 1 Nov. 2020, <https://wiki.ros.org/urdf>